Research Article

SOHAG JOURNAL OF SCIENCES

DOI: 10.21608/sjsci.2025.345701.1244

Analysis of mathematical model for the impact of word of mouth and social media in marketing

Ghada M. El-Sayed[*,1], *Ayman A. Arafa*[1,2], *Ahmed A. Soliman*[1], *and Gamal M. Mahmoud*[3]

[1] Department of Mathematics, Faculty of Science, Sohag University, Sohag 82524, Egypt.
[2] Institute of Basic and Applied Sciences, Egypt-Japan University of Science and Technology, Alexandria, Egypt.
[3] Department of Mathematics, Faculty of Science, Assiut University, Assiut 71516, Egypt.
[*]**Corresponding Author:** ghada.mahmoud@science.sohag.edu.eg.

Received: 21st December 2024, Revised: 15th February 2025, Accepted: 17th February 2025.
Published online: 23th March 2025.

Abstract:

Social media advertising is creating a revolution in digital marketing. It offers businesses an unparalleled and significant opportunity to instantly connect with millions of active users around the world. This paper presents a marketing model that merges two pivotal approaches: direct word-of-mouth promotion and advertisements on social media platforms. The model is used to examine their critical impact on consumer behavior. The existence of steady states is explored through graphical representations of nullclines, and their local stability is examined using the coefficients of the characteristic equation. Our results suggest that the model undergoes a Hopf bifurcation, which highlights the presence of periodic solutions. Additionally, a sensitivity analysis is performed to evaluate how changes in parameters impact clients. Our main findings emphasize the substantial impact of social media advertising on sales. Consequently, the model offers valuable and perceptible insights for developing effective promotional strategies. These strategies drive consumer engagement and increase revenue.
keywords: Social media, marketing, stability, sensitivity analysis, bifurcation.

1 Introduction

Marketing is not only a process but also a driving force that captures consumers' attention, enhances product visibility, and creates unforgettable brand identity. There are numerous methods to market a product or service. This paper focuses on two such methods: direct word-of-mouth and advertisements on social media platforms. Social media has become an integral part of our lives, enabling us to communicate, share content, and gather information on online platforms. These platforms come in various forms, including forums, social networking sites, and bookmarking services. Well-known examples include X, Facebook, Instagram, LinkedIn, Wikipedia, Pinterest, and Google Plus [1,2]. Advertising on social media platforms significantly influences consumers' perceptions of products and their purchasing decisions. Creative advertisements convey compelling ideas that capture attention and spark desire to buy, building brand awareness and implementing measures for long-term profitability. In contrast, short-term strategies typically focus on reducing prices of goods or services to generate immediate revenue [3].

Advertising on social media platforms is widely used to increase product and service awareness, promote brands, retain existing customers, and attract new prospects. Consumers check online reviews to learn more about products and assess companies' credibility, reputation, and background before making purchases. Additionally, social media facilitates knowledge sharing and expertise exchange, accelerating innovation and enabling new product development based on consumer feedback and recommendations. Capitalizing on the surge in online shopping, many businesses, both new and established, have launched promotional activities on social media platforms to enhance brand visibility and boost sales. Given that advertising and word-of-mouth effects are dynamic economic phenomena, numerous studies have utilized the Innovation Diffusion Theory since its emergence in the 1960s, owing to its significant economic relevance [4]. Various mathematical models have been developed to analyze new product marketing, and sales promotions have been extensively examined from both mathematical and economic perspectives. Many of these models focus on explaining new product diffusion [3].

Word-of-mouth (WOM) communication is a widespread and fascinating phenomenon. People can share their experiences about products with their family and friends. Their positive or negative comments impact the purchase decision. WOM network significantly influences the performance of viral marketing [5]. Word-of-mouth equity enables companies to measure how much word-of-mouth communication influences the success of brands and products. For instance, when Apple's iPhone was launched in Germany, its share of word-of-mouth conversations was smaller than that of the market leader. However, the iPhone's influence was much stronger because of the buzz generated by its earlier launches in other countries. Consequently, the iPhone's word-of-mouth equity score jumped up by 30% because three times as many individuals endorsed it compared to competing phones. In this context, sales driven by recommendations of the iPhone exceeded the sales of Apple's paid advertising by some six times. Two years after its release, the iPhone achieved sales of almost 1 million units a year in Germany [6].

Mathematical modelling is systematically representing real-life problems in a mathematical form. This involves solving and analyzing the mathematical problems arising in reality with their interpretation in a logical or applicable model. In the event of direct or simple access to the real object, system, or situation being infeasible, the need for a model becomes apparent. For example, architects resort to building physical models of structures that they wish to build. In the same way, human models wear clothes designed by fashion designers who also create them. In terms of children's toys, cars and trains are toys that depict ordinary objects, which are usually simplified by a mathematical model of complicated systems. These examples show how physical as well as mathematical models transform concepts into workable patterns in a manner that makes it possible to analyze forecasts and make decisions [7]. There are other examples of mathematical modeling, such as ecological balance [8,9]. Our understanding of it is heavily dependent on mathematical models of ecosystems. Forecasting and controlling natural systems, these models assist in establishing conservation strategies and ensuring biodiversity [10,11].

In [12], Feichtinger introduced an advertising diffusion model and investigated how advertising effectiveness influenced goods diffusion between prospective purchasers and clients. Later, Landa improved Feichtinger's model by incorporating the influence of marketing activities and analyzing its dynamic behavior [13]. In [14], Nicoleta analyzed the advertising diffusion model by accounting for a time lag caused by economic, cultural, social, and other influencing factors. In [15], Yang and Zhang developed a stochastic diffusion model that accounted for the impacts of word-of-mouth and advertising on product diffusion. In [16], Paolo et al. employed statistical correlation models to analyze consumer behavior and addressed several methodological challenges in implementing discrete graphical models for market basket analysis data. In [17], Jiang and Ma examined a differential advertising model with internet sales promotions and applied bifurcation theory to determine the conditions for the existence and stability of periodic solutions. In [3], Nie Peidi utilized the logistic curve to describe the change of advertising influence over time. Promotions were considered as factors influencing the stability of differential advertising models by triggering bifurcations and potentially leading to chaotic behavior. In real-world scenarios, when the total cost is fixed, companies can optimize their promotion strategies by adjusting promotional parameters to maximize revenue and, ultimately, profits.

The paper's primary aim is to investigate the impact of word-of-mouth and social media advertisements on consumer behavior simultaneously. We will use the model of Australian scholar Feichtinger [12] and add to it the new compartment that represents advertisements on social media Holling type II. We use the saturation effect because people can't see all advertisements on social media. Our model provides traders with theoretical guidance for taking action in response to changes in the market.

This paper is organized as follows. In Section 2, we design the proposed model based on Feichtinger's advertising diffusion model. Section 3 provides a qualitative analysis of the model. Section 4 presents numerical simulations to deepen our understanding of the model. Finally, Section 5 presents the conclusion of this study.

2 Mathematical model

Word of mouth is a significant factor in impacting consumers' decisions when making purchases. Prior to making a purchase, many consumers make a point to ask for suggestions from friends and family. A favorable recommendation can greatly influence their choice to select a specific product or service. In Feichtinger's advertising diffusion model [12], he assumed that the market's population can be divided into two distinct states: $U(t)$ is the number of prospective purchasers, and $V(t)$ is the number of clients. The model is:

$$\begin{aligned} \frac{dU}{dt} &= k - \alpha U V^2 + bV, \\ \frac{dV}{dt} &= \alpha U V^2 - (b+p)V. \end{aligned} \tag{1}$$

According to his marketing initiatives, he assumed that new individuals were consistently entering the market, becoming prospective customers at an average rate of $k > 0$. He also supposed that $\alpha U V^2$ represents the interaction between prospective purchasers and clients, and α is the rate at which clients attract prospective purchasers. The term V^2 means that the impact of clients on prospective purchasers grows quadratically, so as the number of clients increases, their ability to influence potential buyers grows at an increasing rate. This suggests that having more clients triggers a snowball effect, which significantly increases the number of new prospective purchasers. It was assumed that current customers switched to a competitor brand at a consistent rate of $b > 0$, with the magnitude of this factor being affected by the emergence of other related brands or companies offering similar products. Since individuals had the option to switch back to the original brand, they continued to be part of the potential customer group. Moreover, in a scenario where current customers permanently departed from the market due to mortality, this occurred at a rate of $p > 0$.

Let $u = \frac{\alpha k}{(b+p)p}U$, $v = \frac{p}{k}V$, $\tau = (b+p)t$, $\gamma = \frac{ak^2}{(b+p)p^2}$, $\phi = \frac{b}{(b+p)}$, we get

$$\begin{aligned} \frac{du}{d\tau} &= \gamma - \gamma uv^2 + \gamma\phi(v-1), \\ \frac{dv}{d\tau} &= uv^2 - v. \end{aligned} \tag{2}$$

In today's digital age, marketing products to boost sales relies not solely on word of mouth but also hinges on online advertisements. Hence, our model is designed with the inclusion of a novel compartment $n(t)$ that signifies the number of advertisements on social media platforms. Advertisements on social media platforms motivate individuals to shift from prospective purchasers to consumers at rate $cu\frac{n^2}{n^2+d}$. On the other hand, social media advertising has a naturally limited effect on the public. This is because individuals cannot view all social media advertisements, so a saturated function is utilized. We assume that the growth rate in social media advertising as $r(1-q\frac{v}{v+e})v$, where $q \in (0,1)$. Ads on social media are growing at a rate rv. However, as clients base expand, this r diminishes due to a factor $F(v) = rq\frac{v}{v+e}$ [1]. Over time, the effectiveness of certain social media advertisements in enticing individuals to become customers may diminish. Therefore, social media promotions diminish with a rate of $r_0(n-n_0)$, with n_0 representing a fixed value. Subsequent to these assumptions, the non-linear system transforms into the following:

$$\begin{aligned} \frac{du}{d\tau} &= \gamma - \gamma uv^2 + \gamma\phi(v-1) - cu\frac{n^2}{n^2+d}, \\ \frac{dv}{d\tau} &= uv^2 - v + cu\frac{n^2}{n^2+d}, \\ \frac{dn}{d\tau} &= r(1-q\frac{v}{v+e})v - r_0(n-n_0). \end{aligned} \tag{3}$$

Table (1) provides a detailed description of the parameters for model system (3).

Parameter	Description
k	The influx of prospective purchasers in the market.
a	The influence of Word-of-Mouth on prospective purchasers.
b	The rate of clients converting to prospective purchasers once more.
p	The existing clients exit the market forever.
c	The rate at which clients and prospective purchasers become more aware due to advertisements on social media platforms.
d	Half-saturation point for the impact of social media advertisements on prospective purchasers.
r	Social media advertising growth rate.
q	Decay coefficient in social media ads as a result of rising numbers of customers.
e	Half-saturation point for $F(v)$ as it reaches half of its maximum potential rq when clients arrive at e.
r_0	The decline in social media advertising rates as a result of the inability to encourage people to become clients.
n_0	The number of social media advertisements always maintained by the companies on social sites and is called as baseline number of social media advertisements.

Table 1: A description of the model's parameters

3 Qualitative analysis of *uvn* model (3)

In this section, we investigate the analysis of the *unv* model (2.3), highlighting the positivity and boundedness of the solutions, steady states, and their stability.

Theorem 1. *All solutions of the uvn model (3) with non-negative initial conditions are positive for $\tau \geq 0$.*

Proof. From the second equation of system (3),

$$\frac{du}{d\tau} = uv^2 - v + cu\frac{n^2}{n^2+d}, \tag{4}$$

we claim that $v(\tau) \geq 0$ for all $\tau \geq 0$. Assume contrary, there exists $\tau_1 > 0$ such that $v(\tau_1) = 0$, and $\frac{dv}{d\tau}\big|_{\tau=\tau_1} \leq 0$. Hence, $\frac{dv}{d\tau}\big|_{\tau=\tau_1} = cu(\tau_1)\frac{n(\tau_1)^2}{n(\tau_1)^2+d} \leq 0$. This implies either (i) $u(\tau_1) > 0$ and $\frac{n(\tau_1)^2}{n(\tau_1)^2+d} \leq 0$, or (ii) $u(\tau_1) < 0$ and $\frac{n(\tau_1)^2}{n(\tau_1)^2+d} > 0$. For case (i), this condition is not satisfied because $\frac{n(\tau_1)^2}{n(\tau_1)^2+d} \geq 0$, which results in a contradiction. Therefore, $v(\tau)$ is positive. For case (ii), there exists $\tau_2 \leq \tau_1$ such that $u(\tau_2) = 0$ and $\frac{du}{d\tau}\big|_{\tau=\tau_2} \leq 0$. Hence, $\frac{du}{d\tau}\big|_{\tau=\tau_2} = \gamma(1-\phi) + \gamma\phi v(\tau_2) \leq 0$, but $v(\tau_2) > 0$ and $\phi \in [0,1)$, it follows that $\gamma(1-\phi) + \gamma\phi v(\tau_2) \geq 0$. Therefore, $\frac{du}{d\tau}\big|_{\tau=\tau_2} \geq 0$, which leads to a contradiction, and thus $u(\tau)$ must be positive. Similarly, for the third equation of system (3) there exist $\tau_3 \leq \tau_2 \leq \tau_1$ such that $n(\tau_3) = 0$, and $\frac{dn}{d\tau}\big|_{\tau=\tau_3} \leq 0$. Hence, $\frac{dn}{d\tau}\big|_{\tau=\tau_3} = r(1 - q\frac{v(\tau_3)}{(\tau_3)+e})v(\tau_3) + r_0 n_0 \leq 0$, but $v(\tau_3) > 0$ and $q \in (0,1)$, it follows that $r(1 - q\frac{v(\tau_3)}{(\tau_3)+e})v(\tau_3) \geq 0$. Therefore, $\frac{dn}{d\tau}\big|_{\tau=\tau_3} \geq 0$, which leads to a contradiction, and thus $n(\tau)$ must be positive. This completes the proof.

3.1 Existence and Stability of Steady States

To find the interior equilibrium points for *unv* model (3), we set $\frac{du}{d\tau} = F_1(u,v,n)$, $\frac{dv}{d\tau} = F_2(u,v,n)$ and $\frac{dn}{d\tau} = F_3(u,v,n)$ and then solve $F_1(u,v,n) = F_2(u,v,n) = F_3(u,v,n) = 0$. Due to the difficulty of obtaining fixed points explicitly, we initially assumed that $\gamma = 1$ for the first case and $\gamma \neq 1$ for the second case.

First Case: For $\gamma = 1$

In this case, we obtain a single fixed point $E^0 = (u^0, 1, n^0)$, where

$$u^0 = \frac{(d+(n^0)^2)}{(c+1)(n^0)^2+d},\ n^0 = n_0 + \frac{r(1+e-q)}{r_0(1+e)}. \quad (5)$$

Second Case: For $\gamma \neq 1$

To determine the interior equilibrium points, we need to locate where the three equations in (3) intersect within the positive quadrant. We will accomplish this by identifying the system's nullclines.

From the second equation of (3), we get:

$$u = \frac{(d+n^2)v}{cn^2+(d+n^2)v^2}. \quad (6)$$

Substitute from Eq. (6) into the first equation of (3), we have:

$$n^2(\gamma(v-1)(\phi-1)v^2 + c(-v+\gamma+\gamma\phi(v-1))) + d\gamma(v-1)(\phi-1)v^2 = 0,$$

and the equation's roots are

$$n = \pm\sqrt{\frac{-d\gamma(v-1)(\phi-1)v^2}{(\gamma(v-1)(\phi-1)v^2 + c(-v+\gamma+\gamma\phi(v-1)))}}.$$

From the third equation of (3), we yield

$$n = \frac{e(n_0r_0+rv)+v(n_0r_0-(-1+q)rv)}{r_0(e+v)}.$$

So, we can determine the interior equilibrium points of the system (3), as the intersection points of the following nullclines:

$$n = M_1(v) = \sqrt{\frac{-d\gamma(v-1)(\phi-1)v^2}{(\gamma(v-1)(\phi-1)v^2 + c(-v+\gamma+\gamma\phi(v-1)))}}, \quad (7)$$

$$n = M_2(v) = \frac{e(n_0r_0+rv)+v(n_0r_0-(-1+q)rv)}{r_0(e+v)}. \quad (8)$$

We take the positive square in Eq. (7), if the square root is negative then $n < 0$, and hence there is no branch appearing in the positive quadrant. The function $M_1(v)$ in Eq. (7) is located in the first quadrant of the $v-n$ plan for $v \in [0,1]$. It is increasing at (0,0) and decreasing at (1,0) and $v_{\max} = \frac{1+3\gamma-4\gamma\phi+\sqrt{(1-\gamma)(1-9\gamma+8\gamma\phi)}}{4(1-\gamma\phi)}$ such that $0 < v_{\max} < 1$. In contrast, $M_2(v)$ is an increasing function of v that intersects with the n-axies at $(0,n_0)$. M_2 exists in the first quadrant of the $v-n$ plan for $n \in [0,\infty)$. If we represent the interior equilibrium point as $E_j^*(u_j^*, v_j^*, n_j^*)$ (where j= 1, 2, 3), then u_j^*, v_j^* and n_j^* indicate to the positive solutions for the given equations:

$$n = \frac{e(n_0r_0+rv)+v(n_0r_0-(-1+q)rv)}{r_0(e+v)}, \quad (9)$$

$$u = \frac{(d+n^2)v}{cn^2+(d+n^2)v^2}, \quad (10)$$

and

$$W(v) = a_7v^7 + a_6v^6 + a_5v^5 + a_4v^4 + a_3v^3 + a_2v^2 + a_1v + a_0 = 0, \quad (11)$$

where

$$\begin{aligned}
a_7 &= \gamma r^2(\phi-1)(q-1)^2,\\
a_6 &= -((q-1)r(r(q+2e-1)+2n_0r_0)\gamma(\phi-1)),\\
a_5 &= (er^2(2q+e-2)+2n_0rr_0(-1-e(q-2)+q)\\
&\quad +(d+n_0^2)r_0^2)\gamma(\phi-1)+cr^2(q-1)^2(\gamma\phi-1),\\
a_4 &= \gamma(-2er_0(n_0^2r_0-n_0r(q-2)(\phi-1))\\
&\quad -(d+n_0^2)r_0^2(\phi-1)-e^2r(r-2n_0r_0)(\phi-1))\\
&\quad -c(q-1)r(r\gamma(q-1)(\phi-1)+2er(\gamma\phi-1)\\
&\quad +2n_0r_0(\gamma\phi-1)),\\
a_3 &= er_0\gamma(-2en_0r+r_0(e-2)(d+n_0^2))(\phi-1)\\
&\quad +c(e^2r^2(\gamma\phi-1)+n_0r_0(2r\gamma(q-1)(\phi-1)\\
&\quad +n_0r_0(\gamma\phi-1))+2er(r\gamma(q-1)(\phi-1)\\
&\quad -n_0r_0(q-2)(\gamma\phi-1))),\\
a_2 &= -e^2r_0^2\gamma(d+n_0^2)(\phi-1)\\
&\quad +c(n_0^2r_0^2\gamma(\phi-1)+2en_0r_0(r\gamma(q-2)(\phi-1)\\
&\quad +n_0r_0(\gamma\phi-1)+e^2r(-r\gamma(\phi-1)+2n_0r_0(\gamma\phi-1))),\\
a_1 &= cen_0r_0(-2er\gamma(\phi-1)-2n_0r_0\gamma(\phi-1)\\
&\quad +en_0r_0(\gamma\phi-1)),\\
a_0 &= -ce^2n_0^2r_0^2\gamma(\phi-1).
\end{aligned}$$

It is challenging to determine the intersection point analytically, so we attempt to find these points graphically, as shown in Fig. 1. If we change the values of γ while keeping all other parameters fixed, the number of equilibrium points changes from one to three, as shown in Fig. 1. If we change the values of γ while keeping all other parameters fixed, the number of equilibrium points changes from one to three, as shown in Fig. 1. Fig. 1(a) exhibits that there is unique interior fixed point at $\gamma = \gamma_1 = 0.1$. while when $\gamma = \gamma_2 = 0.09$ the number of interior equilibrium points changes from one to three, as seen in Fig. 1(b).

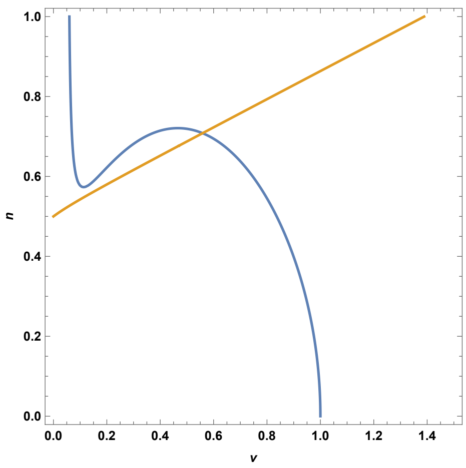

(a)

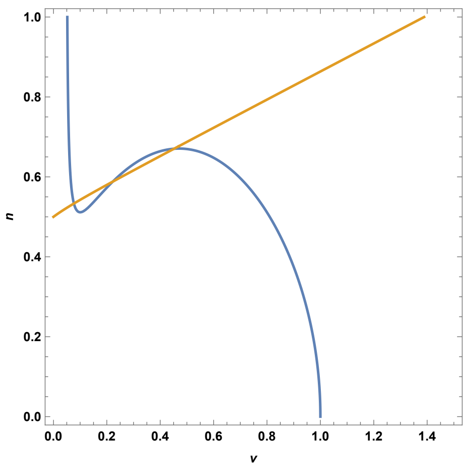

(b)

Figure 1: Graphical representations of nullclines and the number of equilibrium points changes from one to three. [parameters: $\phi = 0.5, c = 0.1, d = 3, r = 0.1, q = 0.3, e = 0.1, r_0 = 0.2, n_0 = 0.5, (a)\gamma_1 = 0.1, (b)\gamma_2 = 0.09$]

3.2 *Local stability of equilibria*

This subsection focuses on examining the local stability of the equilibrium points. Therefore, we determine the Jacobian matrix as follows:

$$J = \begin{pmatrix} F_{1u} & F_{1v} & F_{1n} \\ F_{2u} & F_{2v} & F_{2n} \\ F_{3u} & F_{3v} & F_{3n} \end{pmatrix}, \tag{12}$$

where $F_{1u} = -c\frac{n^2}{n^2+d} - v^2\gamma$, $F_{1v} = \gamma(-2uv + \phi)$, $F_{1n} = -\frac{2cdnu}{(n^2+d)^2}$, $F_{2u} = v^2 + \frac{cn^2}{n^2+d}$, $F_{2v} = 2uv - 1$, $F_{2n} = \frac{2cdnu}{(n^2+d)^2}$, $F_{3u} = 0$, $F_{3v} = r + rq(\frac{e^2}{(e+v)^2} - 1)$, $F_{3n} = -r_0$.

The Jacobian matrix (12) for the first case at E^0 takes the following form:

$$J|_{E^0} = \begin{pmatrix} f_1(n^0) & f_2(n^0) & f_3(n^0) \\ f_4(n^0) & f_5(n^0) & f_6(n^0) \\ 0 & r - rq\frac{(1+2e)}{(e+1)^2} & -r_0 \end{pmatrix}, \tag{13}$$

where $f_1(n^0) = -\frac{c(n^0)^2}{(n^0)^2+d} - \gamma$, $f_2(n^0) = \frac{-2(d+(n^0)^2)}{d+(c+1)(n^0)^2} + \phi$, $f_3(n^0) = -\frac{2cdn^0}{((n^0)^2+d)^2(d+(c+1)(n^0)^2)}$, $f_4(n^0) = 1 + \frac{c(n^0)^2}{(n^0)^2+d}$, $f_5(n^0) = \frac{2(d+(n^0)^2)}{d+(c+1)(n^0)^2} - 1$, $f_6 = \frac{2cdn^0}{((n^0)^2+d)^2(d+(c+1)(n^0)^2)}$.
Consequently, the characteristic equation takes the following form:

$$\lambda^3 + A_2\lambda^2 + A_1\lambda + A_0 = 0, \tag{14}$$

where

$$A_2 = r_0 - (f_1(n^0) + f_5(n^0)),$$
$$A_1 = f_1(n^0)f_5(n^0) - f_2(n^0)f_4(n^0) + f_6(n^0)r\left(\frac{q(1+2e)}{(e+1)^2} - 1\right) - r_0(f_1(n^0) + f_5(n^0)),$$
$$A_0 = r_0(f_1(n^0)f_5(n^0) - f_2(n^0)f_4(n^0)) - \frac{r(f_3(n^0)f_4(n^0) - f_1(n^0)f_6(n^0))((1+e)^2 - q(1+2e))}{(e+1)^2}.$$

Based on the Routh–Hurwitz criterion, the stability of the equilibrium $E^0 = (u^0, 1, n^0)$ depends on the condition that all roots of the characteristic equation have negative real parts. This occurs when $A_i > 0$ for $i = 0$, 1, 2, and $A_2A_1 - A_0 > 0$.

Next, the Jacobian matrix (12) for the second case at E^* is presented as follows:

$$J|_{E^*} = \begin{pmatrix} g_1(v^*,n^*) & g_2(v^*,n^*) & g_3(u^*,n^*) \\ g_4(v^*,n^*) & g_5(u^*,v^*) & g_6(u^*,n^*) \\ 0 & g_7(v^*) & -r_0 \end{pmatrix}, \tag{15}$$

where $g_1(v^*,n^*) = -\frac{c(n^*)^2}{(n^*)^2+d} - (v^*)^2\gamma$, $g_2(v^*,n^*) = \gamma(-2u^*v^* + \phi)$, $g_3(v^*,n^*) = -\frac{2cdn^*u^*}{((n^*)^2+d)^2}$, $g_4(v^*,n^*) = (v^*)^2 + \frac{c(n^*)^2}{(n^*)^2+d}$, $g_5(v^*,n^*) = 2u^*v^* - 1$, $g_6(v^*,n^*) = \frac{2cdn^*u^*}{((n^*)^2+d)^2}$, $g_7(v^*) = r + rq(\frac{e^2}{(e+v^*)^2} - 1)$.
Therefore, the characteristic equation is given by:

$$\lambda^3 + B_2\lambda^2 + B_1\lambda + B_0 = 0, \tag{16}$$

where

$$B_2 = r_0 - (g_1(v^*,n^*) + g_5(v^*,n^*)),$$
$$B_1 = g_1(v^*,n^*)g_5(v^*,n^*) + g_6(v^*,n^*)g_7(v^*) - g_2(v^*,n^*)g_4(v^*,n^*) - r_0(g_1(v^*,n^*) + g_5(v^*,n^*)),$$
$$B_0 = g_3(v^*,n^*)g_4(v^*,n^*)g_7(v^*) + r_0g_1(v^*,n^*)g_5(v^*,n^*) - g_1(v^*,n^*)g_6(v^*,n^*)g_7(v^*) - r_0g_2(v^*,n^*)g_4(v^*,n^*).$$

Therefore, the equilibrium point E^* is stable when $B_i > 0$ for $i = 0$, 1, 2, and $B_2B_1 - B_0 > 0$.

Next, we plot the coefficients of the characteristic equation (16) to identify the number of fixed points and analyze their stability. For $\gamma \in [0, 0.09)$ and $\gamma \in (0.0959, 1.5]$, there is only one fixed point. However, for $\gamma \in [0.09, 0.0959]$, three fixed points are observed in Figs. 2(a), 2(b), 2(c). First, within the range $\gamma \in [0, 0.09)$, we find that B_2, B_0, and $B_2B_1 - B_0$ are positive, indicating that the fixed point in this interval is stable as shown in Fig. 2(a). Secondly, for $\gamma \in [0.09, 0.0959]$, three fixed points emerge. Fig. 2(a) illustrates one of these points has $B_2, B_0 < 0$, and $B_2B_1 - B_0 > 0$ making this fixed point unstable for $\gamma \in [0.09, 0.9464)$. In the interval $\gamma \in [0.9464, 1.5]$ we find that B_2, B_0, and $B_2B_1 - B_0$ are positive, which indicates stability for the fixed point in this range, is stable as shown in Fig. 2(a).

The bifurcation diagram provides insight into how the stability of fixed points shifts as the parameter γ changes, revealing key details about the system's behavior during these transitions. Using XPPAUT software [14], we generate this diagram for our system, with γ as the variable parameter, shown in Fig. 2(d). In the diagram, black lines denote unstable equilibria, while red lines indicate stable equilibria. As γ increases, we initially observe one stable fixed point. With further increases, three fixed points emerge E_1^* and E_2^*, both are unstable and E_3^* is stable. One of these points persists as γ continues to increase. With more increase in γ, this interior point becomes unstable once γ surpasses the first Hopf bifurcation point (HB_1), resulting in the appearance of a stable periodic solution. Interestingly, this point regains stability as γ crosses the second Hopf bifurcation point (HB_2).

Lemma 1. *The unv model (3) has no closed orbits if $r_0 > 1$.*

Proof. Let $P = \{(u,v,n) \in \mathbb{R}_+^3 | u > 0, v > 0, n > 0\}$. Consider the real-valued function

$$G(u,v,n) = \frac{1}{v^2} > 0.$$

lets consider

$$\begin{aligned} H_u &= \gamma - \gamma u v^2 + \gamma \phi (v-1) - cu\frac{n^2}{n^2+d}, \\ H_v &= uv^2 - v + cu\frac{n^2}{n^2+d}, \\ H_n &= r(1 - q\frac{v}{v+e})v - r_0(n-n_0). \end{aligned} \tag{17}$$

Then we have

$$\begin{aligned} &\frac{\partial}{\partial u}(GH_u) + \frac{\partial}{\partial v}(GH_v) + \frac{\partial}{\partial n}(GH_n) \\ &= -\left(\frac{cn^2(2u+v)}{(d+n^2)v^3} + \frac{(d+n^2)v(-1+r_0+v^2\gamma)}{(d+n^2)v^3} \right) < 0, \\ &\text{for } r_0 > 1, \quad \gamma = 1. \end{aligned}$$

According to Dulac's criterion, the *uvn* model (3) has no closed orbits if $r_0 > 1$.

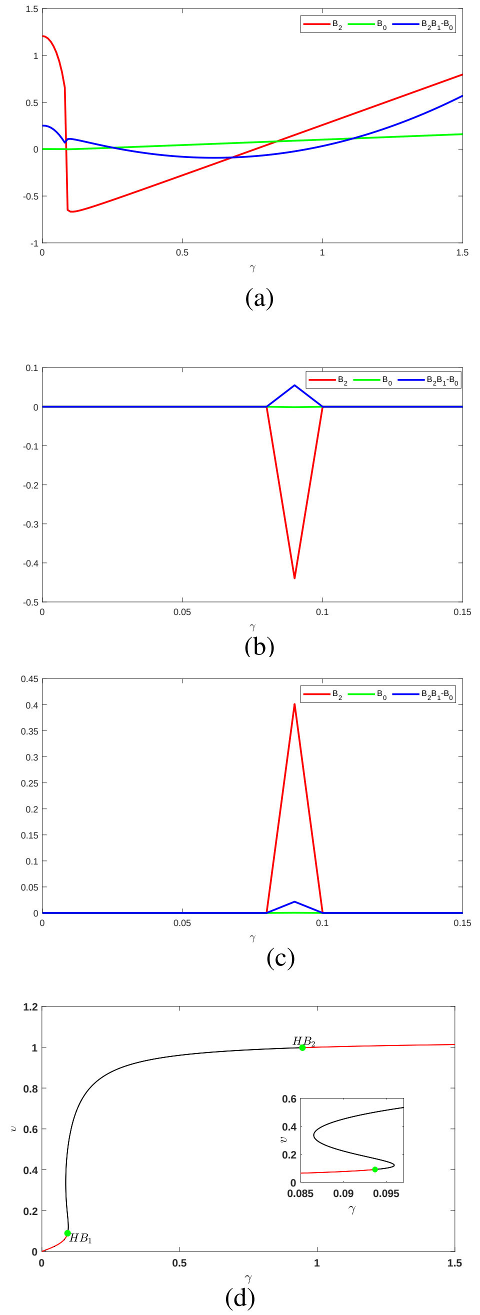

Figure 2: The graphical representations of the coefficients in the characteristic equation (16) for $\gamma \in [0,\ 1.5]$ are presented. Within the interval $\gamma \in [0.09, 0.0959]$, there are three equilibrium points: (a) the first equilibrium point, (b) the second equilibrium point, and (c) the third equilibrium point. (d) The bifurcation diagram for our system is plotted with the parameter γ. The red line represents stable equilibria, while the black line indicates unstable equilibria. The points labeled HB_1 and HB_2 mark the locations of Hopf bifurcations.

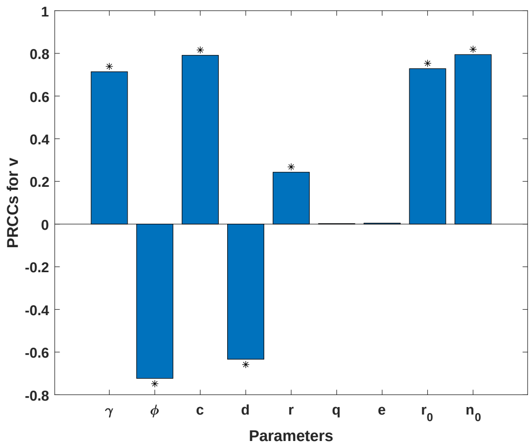

Figure 3: Indicators of sensitivity to buyers (v). Non-zero PRCCs of the parameters are distinguished with $(*)$.

3.3 Sensitivity analysis

This subsection explains the sensitivity analysis of *uvn* model (3), highlighting the key parameters that significantly influence product sales within the context of social media advertising and its effect on marketing dynamics. The core of this analysis is to identify the factors that most significantly influence the model's results, mainly sales volume. We utilize the methodologies of Partial Rank Correlation Coefficient (PRCC) and Latin Hypercube Sampling (LHS) [19,20] to evaluate the impact of various model parameters methodically. We apply these methods to determine the sensitivity of the model's predictions to changes in parameters, amid the inherent uncertainty that characterizes real-world applications [20,21]. Such uncertainty necessitates a thorough analysis to confirm the reliability of the model's predictions. The PRCC values were calculated for the buyers (v) concerning the model's parameters. This analysis is pivotal, as (v) represents the number of consumers who initially are prospective purchasers and later become actual consumers through the influence of social media advertisements. In our analysis, the parameter values are: $\gamma = 0.09, \phi = 0.5, c = 0.1, d = 3, r = 0.1, q = 0.3, e = 0.1, r_0 = 0.2, n_0 = 0.5$. Fig. 3. illustrates that $\gamma, \phi, c, d, r, r_0$ and n_0 exhibit the highest PRCC values. The parameters q and e have a minimal impact on (v). The density of clients increases with an increase in γ, c, r, r_0, and n_0, or decreases in ϕ and d. This is beneficial to increasing sales.

4 Numerical simulation

In this section, we present the numerical simulations conducted to verify the analytical results related to stability conditions using a hypothetical set of parameter systems for nonlinear ordinary differential equations. For the numerical simulation, the parameter values are selected as follows:

$\gamma = 0.09, \phi = 0.5, c = 0.1, d = 3, r = 0.1, q = 0.3, e = 0.1, r_0 = 0.2, n_0 = 0.5$.

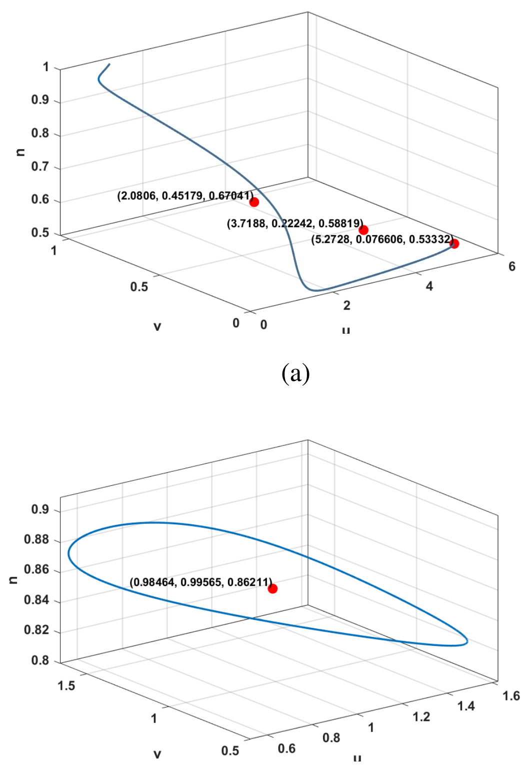

(a)

(b)

Figure 4: Graphical representations of the numerical solutions of the system are shown in 3D space, with fixed points marked in red. The parameters used are: $\phi = 0.5, c = 0.1, d = 3, r = 0.1, q = 0.3, e = 0.1, r_0 = 0.2, n_0 = 0.5$. (a) $\gamma = \gamma_1 = 0.09$, (b) $\gamma = \gamma_2 = 0.9$.

Using the aforementioned parameters, we find that the system exhibits three fixed points: $E_1^*(2.08061, 0.451789, 0.670408), E_2^*(3.71877, 0.222417, 0.588193)$, and $E_3^*(5.27284, 0.0766056, 0.533318)$. At E_1^*, we calculate the numerical values of the coefficients of the characteristic equation (16) using the selected parameter values. The results are $B_2 = -0.648594 < 0, B_1 = -0.165388 < 0$, and $B_0 = -0.0010599 < 0$ with $B_2B_1 - B_0 = 0.10833 > 0$. Similarly, for E_2^*, we obtain $B_2 = -0.439443 < 0, B_1 = -0.122809 < 0$, and $B_0 = -0.00107753 < 0$ with $B_2B_1 - B_0 = 0.0550451 > 0$. Since E_1^* and E_2^* have negative coefficients, they are both unstable. Conversely, E_3^* is stable, as shown by the coefficients $B_2 = 0.40133 > 0, B_1 = 0.054887 > 0$, and $B_0 = 0.000367087 > 0$ with $B_2B_1 - B_0 = 0.0216607 > 0$, as illustrated in Fig. 4(a). Next, if we choose $\gamma = \gamma_2 = 0.9$, the system has a unique fixed point, $E^*(0.98464, 0.995655, 0.86211)$, as illustrated in Fig. 4(b).

By calculating the coefficients of the characteristic equation (16) with the chosen parameter values, we obtain $B_2 = 0.151324 > 0, B_1 = 0.4459440 > 0$, and $B_0 = 0.090372 > 0$ with $B_2 B_1 - B_0 = -0.0228901 < 0$. The Routh–Hurwitz stability criterion is not satisfied by These values. Consequently, the system exhibits a limit cycle around the equilibrium point E^*.

In the context of marketing campaigns, a limit cycle represents a recurring pattern in the dynamics of prospective purchasers and client interactions, driven by the interplay between social media advertisements and word-of-mouth (WOM) marketing. As a catalyst, social media ads pique consumers' interest and start conversations that spread word-of-mouth. WOM creates a natural buzz that keeps the campaign's influence going after its active phase as customers share their experiences, increasing the reach and efficacy of ads. After a while, both WOM and advertising become saturated, which causes engagement to drop until a new stimulus, like a new campaign, sparks interest again. The idea of a limit cycle is mirrored in this periodic pattern that demonstrates the dynamic synergy between advertising and WOM. The graph is an effective tool for understanding the relationships between prospective purchasers, clients, and advertisements on social media. Marketers can enhance engagement, increase conversions, and ultimately increase sales by examining these links and adjusting their tactics accordingly. In addition to increasing marketing efficacy right away, this data-driven strategy creates the framework for future expansion and client loyalty. Businesses can adjust and improve their marketing efforts by utilizing the graph's data, guaranteeing that they reach and surpass their sales goals.

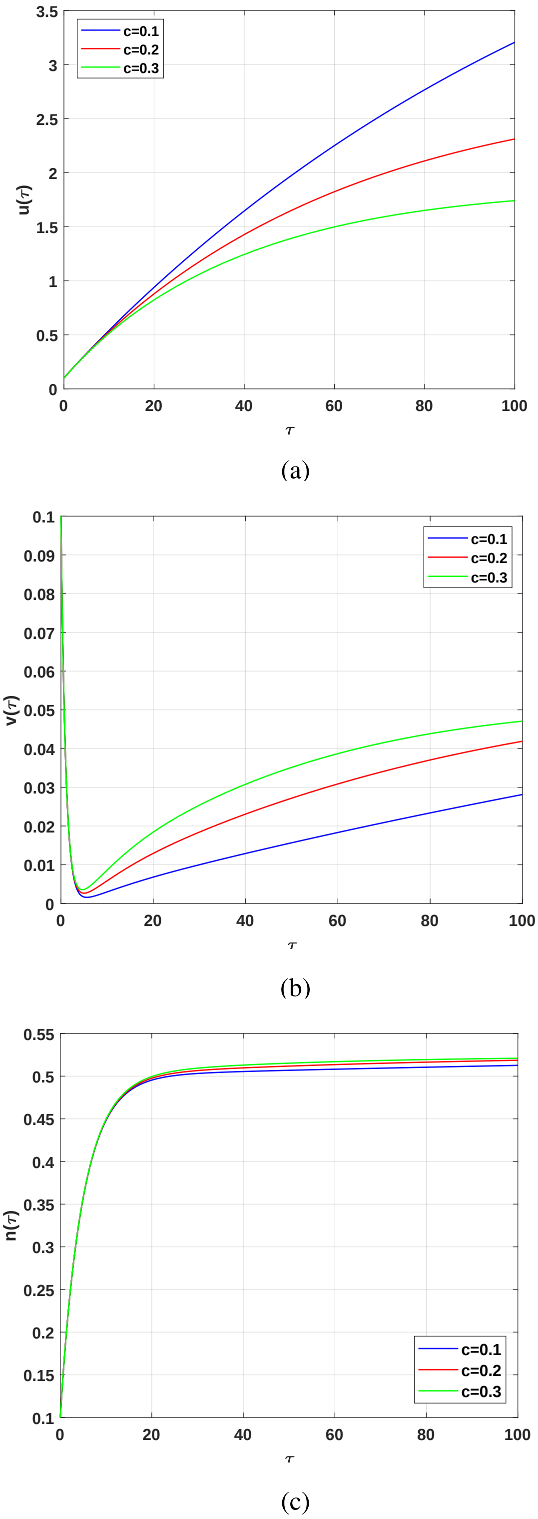

Figure 5: Plots illustrating the variation of $u(\tau), v(\tau)$ and $n(\tau)$ with respect to time τ for various values of c.

We now analyze the impact of the advertisement rate on social media platforms, c, on system dynamics for various values. Figs. 5(a), 5(b), and 5(c) illustrate the variation of

$u(\tau)$, $v(\tau)$, and $n(\tau)$ with respect to time τ for different values of c. These plots reveal that as c increases, the density of prospective purchasers $u(\tau)$, decreases, while the densities of clients $v(\tau)$ and social media advertisements $n(\tau)$ rise. The higher the value of c, the greater the conversion of potential consumers into clients, indicating the existence of market sales because of intensified social media advertisement activities. Therefore, parameter c is one of the most important factors determining the dynamics of prospective purchasers and clients. Higher values of c more average awareness increase prospective purchaser's density and actual conversion rates into clients. Firms need to redirect their marketing resource allocations towards making advertising strategies that give more attention to enhancing customer awareness, thus eventually leading to better marketing performance and sales.

Fig. 6 illustrates the variation of $u(\tau), v(\tau)$ and $n(\tau)$ for different values of r_0. As shown in Fig. 6(a), the density of prospective purchasers, $u(\tau)$, increases, which indicates that fewer individuals are being attracted to the product due to ineffective advertising strategies. This trend stems from a reduction in social media advertising rates, represented by r_0, which fails to effectively convert individuals into clients. At the beginning of the marketing campaign, the density of clients and social media advertisements increases. As r_0 rises beyond the advertisements diminish, leading to a decline in both client density and social media advertisements, as depicted in Figs. 6(b) and 6(c). Also as social media advertising rates go down, sales can rise with organic engagement and word-of-mouth, which can drive higher conversion rates. With less advertising, the company can develop more targeted and personalized campaigns that reach an increasingly interested audience, further driving up sales.

Finally, we examine how $u(\tau), v(\tau)$, and $n(\tau)$ are affected by the baseline number of social media ads n_0. It refers to the initial or standard number of ads displayed on social media platforms before any changes or adjustments in strategy or advertising budget. This figure is used as a reference to compare the impact of modifications to advertising campaigns. Figure 7(a) depicts how the density of prospective buyers, $u(\tau)$, reduces as n_0 rises. while both the density of clients, $v(\tau)$, and the number of advertisements on social media platforms, $n(\tau)$, increase, as shown in Figs. 7(b) and 7(c). This suggests that sales improve as the baseline number of social media advertisements, n_0, rises, attracting more individuals to become clients. The dynamics between prospective purchasers and clients are significantly shaped by the baseline quantity of social media ads, n_0. Higher values of n_0 lead to increased visibility, higher conversion rates, and more effective advertising strategies. Therefore, companies should prioritize maintaining an optimal baseline of advertisements to maximize marketing outcomes and guarantee steady audience engagement.

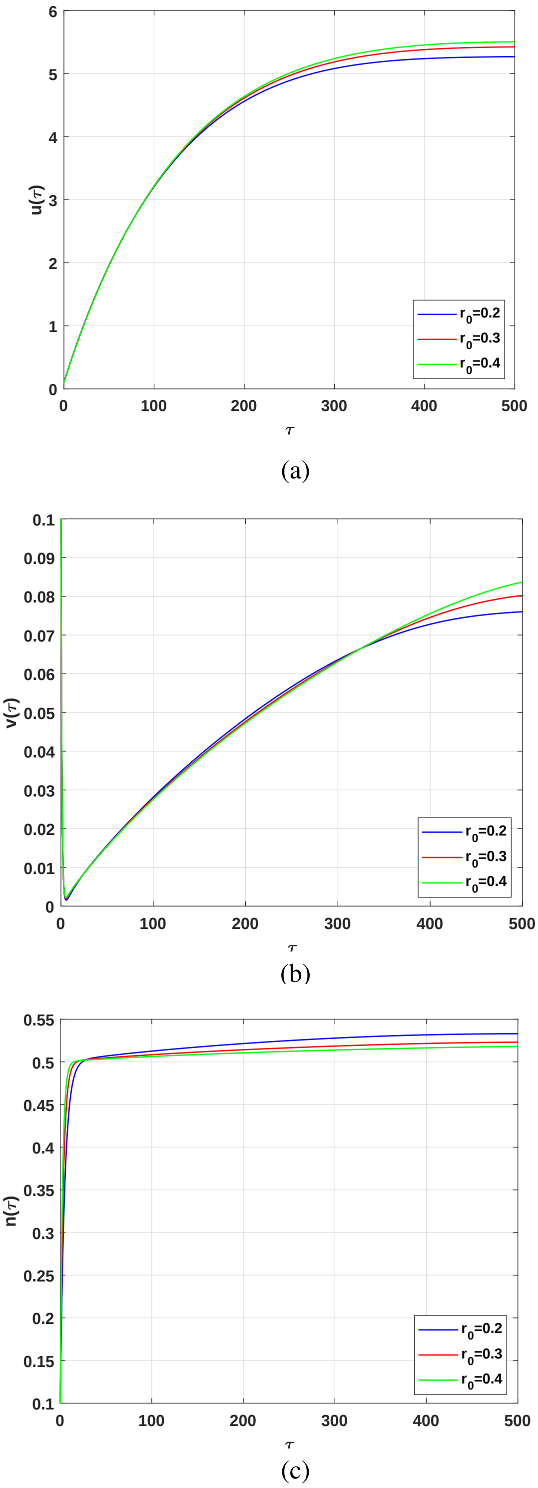

Figure 6: Plots illustrating the variation of $u(\tau), v(\tau)$ and $n(\tau)$ with respect to time τ for various values of r_0.

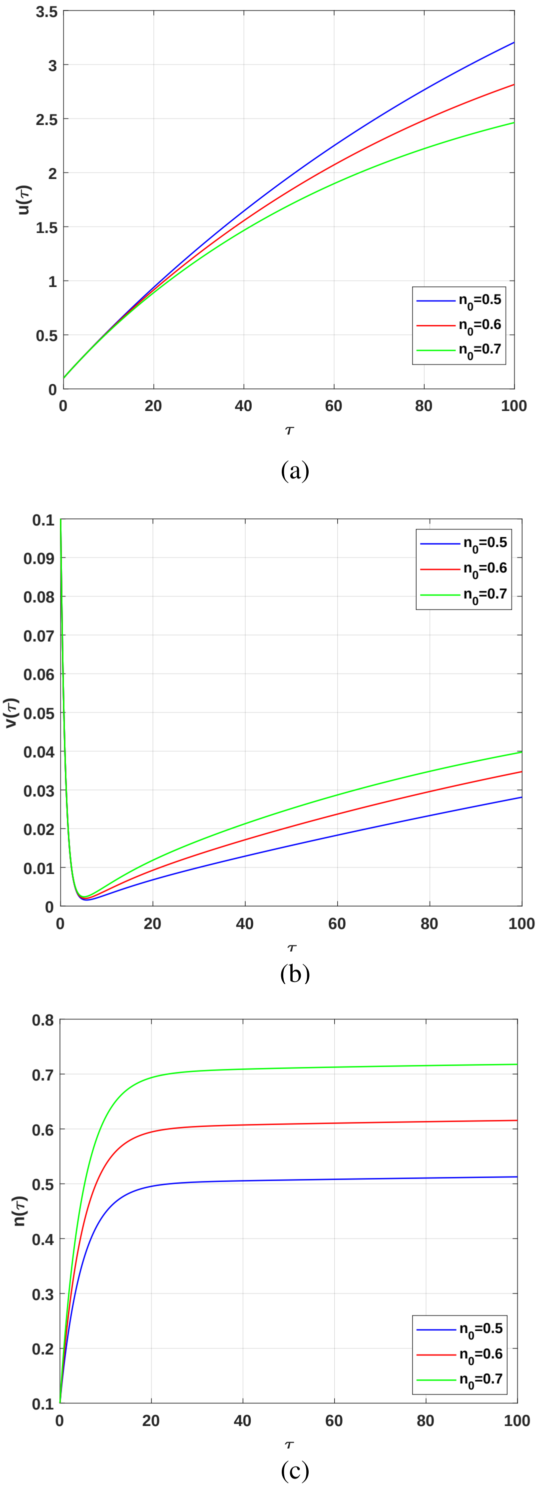

Figure 7: Plots illustrating the variation of $u(\tau), v(\tau)$ and $n(\tau)$ with respect to time τ for various values of n_0.

5 Conclusions

Social media has brought changes in people's lives, as they use these platforms for a variety of purposes, including communication, e-business, and buying and selling. Advertising on social media platforms effectiveness and word-of-mouth continue to play a vital role in shaping consumer behavior and influencing market trends. Its ability to spread information and influence people's decisions ensures its ongoing significance in the business world. It passes traditional advertising by providing a more authentic and trustworthy mode of communication. Based on the advertising diffusion model [12], we have formulated our model to incorporate the impact of advertising on social media platforms and word-of-mouth in consumers' decisions.

In our model, consumers can be classified into four distinct categories: prospective purchasers (U), actual purchasers (V), and advertisements on social media platforms (n). An essential part of our model examines the consequences of advertising and word-of-mouth effects on consumer behavior. The graphical representations of nullclines have provided insights into the number of equilibria present. It has shown that the number of equilibrium points changed from one to three. The stability of each equilibrium point has been assessed through graphical representations of the coefficients in the characteristic equation. Additionally, we have explored the dynamics associated with the Hopf bifurcation. According to Dulac's criterion, the model (3) has no closed orbits if $r_0 > 1$. A normalized sensitivity analysis was performed to determine the most sensitive parameters and their impact on clients. It was found that the density of clients increases with an increase in γ, c, r, r_0, and n_0, or decreases with ϕ and d.

Numerical simulations in our model exhibited how parameter changes significantly affect consumer behavior and illustrate the impact of social media advertising on market dynamics. As the value of c rises, the conversion rate of prospective purchasers into clients increases, signaling a more dynamic market and driving sales growth through intensified social media advertising efforts. On the other hand, the density of clients increases as r_0 rises; however, beyond a certain point, the effectiveness of the advertisements diminishes, leading to a decline in client density. This suggests that sales grow when social media campaigns successfully convert individuals into clients but decline when these advertisements lose their impact. As n_0 increases, it leads to an increase in the number of clients. The baseline number of social media advertisements, n_0, plays a crucial role in shaping the dynamics between prospective and actual buyers.

Our findings validate the model's effectiveness and emphasize the crucial role of parameters such as c, r_0, and n_0 in shaping the outcomes of social media advertising and marketing strategies. By comprehending these impacts, companies should focus on refining their advertising strategies to capitalize on social media advertisements to enhance client awareness, ultimately driving better marketing outcomes and increased sales.

CRediT authorship contribution statement

Author Contributions: For research articles with several authors, a short paragraph specifying their individual contributions must be provided. The following statements should be used "Conceptualization, G.M.E. and A.A.A.; methodology, G.M.E. and A.A.A.; software, G.M.E. and A.A.A.; writing—original draft preparation, G.M.E.; writing—review and editing, G.M.E., A.A.A., A.A.S. and G.M.M.; supervision, A.A.A., A.A.S. and G.M.M. All authors have read and agreed to the published version of the manuscript."

Acknowledgments

The authors are grateful to the Faculty of Science for its support in publishing this work.

Conflict of interest

The authors declare no conflicts of interest regarding the publication of this paper

References

[1] A. K. Misra, K. Goyal, and J. Maurya, Differential Equations and Dynamical Systems, 31 (2023) 651-671.
[2] G. Hegde, G. Shainesh (eds.), Palgrave Macmillan, (2018).
[3] P. Nie, et al., J. Nonlinear Model. Anal., 1 (2019) 461-489.
[4] L. Lambert, C. Woodford, and C. J. Moschovitis, ABC-CLIO, (2005).
[5] P. Li, et al., Physica A: Statistical Mechanics and its Applications, 493 (2018) 1-16.
[6] J. Bughin, J. Doogan, and O. J. Vetvik, McKinsey Quarterly, 2 (2010) 113-116.
[7] S. Dundar, B. Gokkurt, and Y. Soylu, in Proc. of Procedia-Social and Behavioral Sciences, 46 (2012) 3465-3470.
[8] S. A. A. Hamdallah, and A. A. Arafa, Journal of Applied Mathematics and Computing, 70 (2024) 73-102.
[9] D. M. Fawzy, et al., Applied Mathematics and Computation, 480 (2024) 128908.
[10] D. M. Fawzy, et al., Chaos: An Interdisciplinary Journal of Nonlinear Science, 33 (2023).
[11] S. A. A. Hamdallah, et al., International Journal of Bifurcation and Chaos, 31 (2021) 2150074.
[12] G. Feichtinger, Journal of Economic Behavior and Organization, 17 (1992) 401–411.
[13] F. J. Landa Bercebal, F. Velasco Morente, and L. González Abril, Innovar, 25 (2015) 107–120.
[14] N. Sirghi and M. Neamtu, WSEAS Transactions on System and Control, 4 (2013) 141–150.
[15] C. Yang and C. Zhang, Institute of Electrical and Electronics Engineers, 15 (2015) 1530–1605.
[16] P. Giudici and G. Passerone, Computational Statistics & Data Analysis, 38 (2002) 533–541.
[17] H. Jiang and J. Ma, Discrete Dynamics in Nature and Society, 2018 (2018) 8618146.
[18] B. Ermentrout and A. Mahajan, Appl. Mech. Rev., 56 (2003) B53-B53.
[19] E. Chikaki and H. Ishikawa, The Journal of Infection in Developing Countries, 3 (2009) 711–722.
[20] S. Marino, I. B. Hogue, C. J. Ray, and D. E. Kirschner, Journal of Theoretical Biology, 254 (2008) 178–196.
[21] S. M. Blower and H. Dowlatabadi, International Statistical Review/Revue Internationale de Statistique, (1994) 229–243.